



Antimony(V) catecholato complexes based on 4,5-dialkylsubstituted *o*-benzoquinone. The spectroscopic and electrochemical studies. Crystal structure of $[\text{Ph}_4\text{Sb}]^+[\text{Ph}_2\text{Sb}(4,5\text{-Cat})_2]^-$

Andrey I. Poddel'sky^{a,*}, Ivan V. Smolyaninov^b, Nikolay V. Somov^c, Nadezhda T. Berberova^b, Vladimir K. Cherkasov^a, Gleb A. Abakumov^a

^aG.A. Razuvaev Institute of Organometallic Chemistry, Russian Academy of Sciences, Tropinina 49, 603950 Nizhny Novgorod, GSP-445, Russia

^bSouthern Scientific Center, Russian Academy of Sciences, 41 Chekhova Street, 344006 Rostov-on-Don, Russia

^cNizhny Novgorod State University, Physical Faculty, Building 3, Gagarina Avenue 23, 603950 Nizhny Novgorod, Russia

ARTICLE INFO

Article history:

Received 29 May 2009

Received in revised form 3 November 2009

Accepted 16 November 2009

Available online 23 November 2009

Keywords:

Antimony

o-Quinone

Catecholates

NMR spectroscopy

X-ray structure

Electrochemistry

ABSTRACT

Triphenylantimony(III) and triethylantimony(III) readily react with 4,5-(1,1,4,4-tetramethyl-butane-1,4-diyl)-*o*-benzoquinone to form catecholato complexes $\text{R}_3\text{Sb}(4,5\text{-Cat})$ ($\text{R} = \text{Ph}$ (**1**), Et (**2**); 4,5-Cat is dianionic 4,5-(1,1,4,4-tetramethyl-butane-1,4-diyl)-catecholates). In polar solvents (CHCl_3 , acetone) complex **1** transforms easily to ionic complex compound $[\text{Ph}_4\text{Sb}]^+[\text{Ph}_2\text{Sb}(4,5\text{-Cat})_2]^-$ (**3**) with diphenyl-bis-[4,5-(1,1,4,4-tetramethyl-butane-1,4-diyl)-catecholato]antimony(V) complex anion. Complexes were characterized by IR, ^1H , ^{13}C NMR spectroscopy, cyclic voltammometry. Molecular structure of **3**· CHCl_3 was confirmed by X-ray analysis. Cyclic voltammometry of **1** and **3** shows that both complexes undergo reversible one-electron oxidation to quite stable paramagnetic *o*-semiquinonato species $[\text{Ph}_3\text{Sb}(4,5\text{-SQ})]^+$ and $[\text{Ph}_2\text{Sb}(4,5\text{-SQ})(4,5\text{-Cat})]$ (0.75 and 0.49 V in CH_2Cl_2 vs. $\text{Ag}/\text{AgCl}/\text{KCl}$, respectively).

© 2009 Elsevier B.V. All rights reserved.

1. Introduction

At the present time the coordination and organometallic chemistry of antimony(III, V) becomes a dynamic developed area of chemistry. Organoantimony compounds attract the scientists' interest owing to their activity in quite a number of reactions [1–6], fine organic synthesis [7–13]. Antimony organics have found their application in pharmacy and medicine (as the medicaments, antioxidants), agriculture (fungicides), etc. [14–16]. The combination of antimony and redox-active *o*-quinone type ligands have revealed next one unusual property of non-transition metal complexes – the reversible binding of molecular oxygen [17–19]. These circumstances cause our interest to new antimony complexes with *o*-quinonato type ligands which can serve as oxidizing agents, dioxygen carriers etc.

In our previous investigations we have synthesized a number of triphenylantimony(V) catecholates of different sterically hindered di-*tert*-butyl-*o*-quinones [18,20,21]. It was shown that the structure and stability of complexes formed depends on sterical shielding of Cat ligand as well as redox-potentials of Cat ligand [21]. For example, the application of catecholates with electron-donor

groups 4-methoxy- or 4,5-dimethoxy-3,6-di-*tert*-butyl-catecholate (4-MeO- and 4,5-(MeO)₂-3,6-DBCat) allows these complexes to reversibly trap molecular oxygen [18], while the insertion of different acceptors to Cat ligand results in air-stable catecholates [20,21]. What about sterical factors, in most cases catecholates used are derivatives of sterically hindered 3,6-di-*tert*-butyl-*o*-benzoquinone or 3,5-di-*tert*-butyl-*o*-benzoquinone. Here we report synthesis and structure of new antimony(V) catecholates based on 4,5-dialkylsubstituted *o*-benzoquinone 4,5-(1,1,4,4-tetramethyl-butane-1,4-diyl)-*o*-benzoquinone which has not hindrances at 3 and 6 positions of Cat ligand and it leads to some chemical features of complexes formed. We can expect some reactivity of complexes in dioxygen binding reaction and their ability to undergo the rearrangement to form bis-catecholato-diphenylantimonato(V) anionic salts.

2. Experimental

All manipulations were carried out under an air-free atmosphere. All solvents were purified using standard technique [22]. Anhydrous SbCl_3 , SbPh_3 and EtBr were purchased. SbEt_3 [23], 4,5-(1,1,4,4-tetramethyl-butane-1,4-diyl)-*o*-benzoquinone [24] were prepared according to reported procedures.

* Corresponding author. Fax: +7 831 462 74 97.

E-mail address: aip@iomc.ras.ru (A.I. Poddel'sky).

2.1. Synthesis

2.1.1. (4,5-(1,1,4,4-tetramethyl-butane-1,4-diyl)-catecholato)triphenylantimony(V) (1)

A toluene solution of 4,5-(1,1,4,4-tetramethyl-butane-1,4-diyl)-*o*-benzoquinone (0.219 g, 1 mmol, 20 ml) was added with a continuous stirring to a toluene solution of SbPh₃ (0.354 g, 1 mmol, 15 ml). After the solution color changed to bright yellow, toluene was replaced with hexane. Storing of the solution at –18 °C allowed to form precipitate bright yellow powder which was filtered off and dried in vacuo. Yield is 0.45 g (78.7%), m.p. 129–133 °C. *Anal. Calc.* for C₃₂H₃₃O₂Sb: C, 67.27; H, 5.82; Sb, 21.31. Found: C, 66.98; H, 5.90; Sb, 21.48%. IR (nujol, ν , cm⁻¹): 1604 w, 1570 w, 1492 s, 1458 m, 1435 s, 1402 w, 1377 m, 1360 m, 1340 m, 1307 w, 1254 s, 1207 m, 1181 m, 1158 m, 1099 w, 1084 w, 1067 m, 1022 m, 997 m, 889 m, 870 s, 814 s, 782 w, 741 s, 693 s, 663 w, 654 w, 616 w, 588 m, 567 m, 543 w, 527 m, 453 s. ¹H NMR (CDCl₃, δ , ppm): 1.24 (s, 12H, 4CH₃), 1.64 (s, 4H, –CH₂–CH₂–), 6.89 (s, 2H, C₆H₂), 7.38–7.52 (m, 9H, SbPh₃), 7.70–7.77 (m, 6H, SbPh₃). ¹H NMR (d⁸-acetone, δ , ppm): 1.20 (s, 12H, 4CH₃), 1.62 (s, 4H, –CH₂–CH₂–), 6.69 (s, 2H, C₆H₂), 7.42–7.58 (m, 9H, SbPh₃), 7.70–7.86 (m, 6H, SbPh₃). ¹³C NMR (CDCl₃, δ , ppm): 32.11 (CH₃), 33.90 (C(CH₃)₂), 35.52 (–CH₂–CH₂–), 109.46 (CH of Ar), 129.22 (SbPh₃), 131.15 (SbPh₃), 134.71 (Ar), 135.03 (SbPh₃), 137.71 (SbPh₃), 145.39 (Ar). ¹³C{¹H} NMR (CDCl₃, δ , ppm): 32.11, 35.52, 109.46, 129.22, 131.15, 135.03. ¹³C NMR (d⁸-acetone, δ , ppm): 32.55 (CH₃), 34.40 (C(CH₃)₂), 36.40 (–CH₂–CH₂–), 109.99 (CH of Ar), 129.80 (SbPh₃), 131.56 (SbPh₃), 134.74 (Ar), 135.75 (SbPh₃), 140.99 (SbPh₃), 146.68 (Ar). ¹³C{¹H} NMR (CDCl₃, δ , ppm): 32.55, 36.40, 109.99, 129.80, 131.56, 135.75.

2.1.2. (4,5-(1,1,4,4-tetramethyl-butane-1,4-diyl)-catecholato)triethylantimony(V) (2)

Complex **2** was prepared by the same method as reported for **1** from 0.21 g (1 mmol) of SbEt₃ and 0.22 g (1 mmol) of 4,5-(1,1,4,4-tetramethyl-butane-1,4-diyl)-*o*-benzoquinone. Complex was isolated from pentane. Yield is 0.28 g (65.6%), decomp. >100 °C. *Anal. Calc.* for C₂₀H₃₃O₂Sb: C, 56.23; H, 7.79; Sb, 28.50. Found: C, 56.71; H, 7.90; Sb, 27.88%. IR (nujol, ν , cm⁻¹): 1608 w, 1589 w, 1513 w, 1493 s, 1463 m, 1404 w, 1364 w, 1341 w, 1318 w, 1273 s, 1252 s, 1206 m, 1160 m, 1150 m, 1084 w, 1020 m, 989 w, 890 w, 876 w, 860 m, 812 m, 805 m, 722 m, 690 w, 557 w, 407 m. ¹H NMR (CDCl₃, δ , ppm): 1.22 (s, 12H, 4CH₃), 1.39 (t, ⁴J_{HH} = 7.9 Hz, 9H, 3 CH₃CH₂), 1.63 (s, 4H, –CH₂–CH₂–), 1.96 (q, ⁴J_{HH} = 7.9 Hz, 6H, 3 CH₃CH₂), 6.71 (s, 2H, C₆H₂). ¹³C NMR (CDCl₃, δ , ppm): 9.13 (CH₃CH₂), 19.99 (CH₃CH₂), 32.09 (CH₃), 33.85 (C(CH₃)₂), 35.57 (–CH₂–CH₂–), 108.91 (CH of Ar), 134.09 (Ar), 145.89 (Ar). ¹³C{¹H} NMR (CDCl₃, δ , ppm): 9.13, 19.99, 32.09, 35.57, 108.91.

2.1.3. Tetraphenylstibonium(V) diphenyl-bis-[4,5-(1,1,4,4-tetramethyl-butane-1,4-diyl)-catecholato]antimony(V) (3)

A sample of complex **1** (0.05 g, 0.087 mmol) was dissolved in CHCl₃ (10 ml) and left untouched for a week. The yellow color of solution disappeared slowly with concomitant formation of nearly colorless crystals suitable for X-ray analysis. Yield of **3**·CHCl₃ is 0.053 g (96%). *Anal. Calc.* for C₆₅H₆₇Cl₃O₄Sb₂: C, 61.86; H, 5.35; Cl, 8.43; Sb, 19.29. Found: C, 61.53; H, 5.27; Cl, 8.01; Sb, 19.43%.

IR (nujol, ν , cm⁻¹): 1604 w, 1490 m, 1462 m, 1437 m, 1377 m, 1356 w, 1340 w, 1306 w, 1246 s, 1203 w, 1183 w, 1156 w, 1102 w, 1077 w, 1066 m, 1019 w, 995 m, 929 w, 891 w, 871 s, 861 s, 810 s, 781 w, 731 s, 700 s, 689 s, 661 w, 657 w, 639 w, 583 m, 567 w, 543 w, 518 w, 456 s, 444 s, 409 w.

¹H NMR (d⁸-acetone, δ , ppm): 1.07 (s, 6H, 2 CH₃), 1.10 (s, 6H, 2 CH₃), 1.16 (s, 6H, 2 CH₃), 1.20 (s, 6H, 2 CH₃), 1.56 (s, 8H, –CH₂–CH₂–), 6.29 (s, 2H, C₆H₂), 6.63 (s, 2H, C₆H₂), 7.14–7.22 (m, 6H, 2

p-H, 4 *o*-H of SbPh₂), 7.68–7.85 (m, 16H, 4 *m*-H of SbPh₂ and 4 *p*-H, 8 *o*-H of SbPh₄), 7.89–7.96 (m, 8H, *m*-H of SbPh₄).

¹³C NMR (d⁸-acetone, δ , ppm): 32.51, 32.58, 32.61, 32.78 (all CH₃), 34.19 and 34.21 (both C(CH₃)₂), 36.72 and 36.74 (–CH₂–CH₂–), 110.25 and 110.34 (both CH of Ar), 128.17 (*o*-C of SbPh₂), 128.81 (*p*-C of SbPh₂), 131.51 (Ar), 131.86 (*m*-C of SbPh₄⁺), 133.12 (Ar), 134.49 (*p*-C of SbPh₄⁺), 134.73 (*m*-C of SbPh₂), 135.73 (*i*-C of SbPh₂), 136.62 (*o*-C of SbPh₄⁺), 149.09 (Ar), 150.36 (Ar), 151.92 (*i*-C of SbPh₄⁺). ¹³C{¹H} NMR (CDCl₃, δ , ppm): 32.51, 32.58, 32.61, 32.78, 36.72, 36.74, 110.25, 110.34, 128.17, 128.81, 131.86, 134.49, 134.73, 136.62.

2.2. Physical measurements

Bruker AVANCE DPX-200 spectrometer was used for recording the ¹H, ¹³C, ¹³C DEPT NMR spectra. Chemical shifts for ¹H and ¹³C spectra were referenced internally according to the residual solvent resonances and reported relative to TMS; CDCl₃ and d⁸-acetone were used as solvents. Infrared spectra were recorded on a Perkin–Elmer FT-IR spectrometer as Nujol mulls and are reported in cm⁻¹.

Electrochemical studies were carried out using an IPC-pro potentiostat in threeelectrode mode. The glassy carbon (*d* = 2 mm) disk was used as working electrode; the auxiliary electrode was a platinum-flag electrode. The reference electrode was an Ag/AgCl/KCl (sat.) with watertight diaphragm. All measurements were carried out under argon. The samples were dissolved in the pre-deaerated solvent. The rate scan was 200 mV s⁻¹. The supporting electrolyte 0.1 M [(*n*-Bu)₄N]ClO₄ (99%, “Acros”) was doubly recrystallized from aqueous ethanol and then it was dried in vacuum at 50 °C for 48 h.

2.3. Crystal structure determination

X-ray diffraction data for **3**·CHCl₃ were collected by using Oxford Diffraction (Gemini S) diffractometer with graphite monochromated Mo K α radiation (λ = 0.71073 Å) and with CCD detector Sapphire III in the ω -scan mode (hemisphere with max 2θ = 61° resolution, exposure 10 s on each frame). The crystal structure was solved by direct methods (SHELX97) [25] and refined by full matrix method (WINGX and SHELX97) [26]. The reflection data were processed by using the analytical absorption correction algorithm [27]. All non-hydrogen atoms were refined with anisotropic correction. All of H atoms were placed in calculated positions and refined in the “riding-model” ($U_{iso}(H)$ = 1.2 $U_{eq}(\text{carbon})$ Å² for aromatic hydrogen and 1.5 $U_{eq}(\text{carbon})$ Å² for alkyl hydrogen). The follow minimal *R*₁-factor was obtained for **3**·CHCl₃ is *R*₁ = 0.0295. The selected bond lengths and angles are listed in Table 1. Crystallographic data on **3**·CHCl₃ are given in Table 2.

3. Results and discussion

3.1. Synthesis and characterization

The oxidative addition of 4,5-(1,1,4,4-tetramethyl-butane-1,4-diyl)-*o*-benzoquinone to triphenylstibine or triethylstibine (Scheme 1) proceeds easy with the color change from orange-red (the color of initial quinone) to bright yellow. The reaction product, (4,5-(1,1,4,4-tetramethyl-butane-1,4-diyl)-catecholato)triphenylantimony(V) (**1**), is slightly soluble in a wide number of polar and non-polar solvents.

Complexes were characterized by ¹H and ¹³C NMR-, IR-spectroscopy and an elemental analysis.

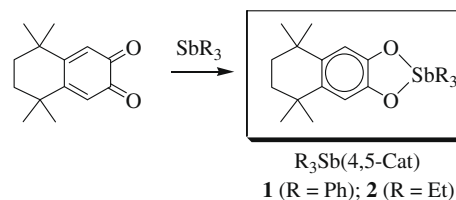
Compound **1** was found to be air-stable like the related complex (3,6-di-tert-butyl-catecholato)triphenylantimony [20]. The tri-

Table 1
Selected bond distances (Å) and bond angles (°) in **3**·CHCl₃.

Bond distances (Å)	Bond angles (°)
Sb(1)–C(29) 2.146(2)	C(2)–O(2)–Sb(1) 111.37(13)
Sb(1)–C(35) 2.134(2)	C(15)–O(3)–Sb(1) 110.36(13)
Sb(2)–C(41) 2.095(2)	C(1)–O(1)–Sb(1) 110.74(13)
Sb(2)–C(47) 2.091(2)	C(16)–O(4)–Sb(1) 110.87(13)
Sb(2)–C(53) 2.100(2)	
Sb(2)–C(59) 2.099(2)	O(4)–Sb(1)–O(2) 164.77(6)
Sb(1)–O(1) 2.0657(16)	O(4)–Sb(1)–O(3) 82.78(6)
Sb(1)–O(2) 2.0297(16)	O(2)–Sb(1)–O(3) 86.36(6)
Sb(1)–O(3) 2.0430(16)	O(4)–Sb(1)–O(1) 86.66(6)
Sb(1)–O(4) 2.0192(16)	O(2)–Sb(1)–O(1) 81.70(6)
C(1)–O(1) 1.353(3)	O(3)–Sb(1)–O(1) 84.59(7)
C(2)–O(2) 1.359(3)	O(4)–Sb(1)–C(35) 91.45(8)
C(15)–O(3) 1.351(3)	O(2)–Sb(1)–C(35) 97.44(8)
C(16)–O(4) 1.364(3)	O(3)–Sb(1)–C(35) 169.10(8)
C(1)–C(2) 1.416(3)	O(1)–Sb(1)–C(35) 85.86(8)
C(1)–C(10) 1.378(3)	O(4)–Sb(1)–C(29) 94.89(8)
C(2)–C(3) 1.379(3)	O(2)–Sb(1)–C(29) 95.95(8)
C(3)–C(4) 1.412(3)	O(3)–Sb(1)–C(29) 91.03(8)
C(4)–C(9) 1.403(3)	O(1)–Sb(1)–C(29) 175.14(8)
C(4)–C(5) 1.528(3)	C(35)–Sb(1)–C(29) 98.69(9)
C(5)–C(6) 1.534(4)	
C(6)–C(7) 1.514(4)	C(47)–Sb(2)–C(41) 105.17(9)
C(7)–C(8) 1.531(4)	C(47)–Sb(2)–C(59) 114.21(9)
C(8)–C(9) 1.537(3)	C(41)–Sb(2)–C(59) 108.37(9)
C(9)–C(10) 1.401(3)	C(47)–Sb(2)–C(53) 113.23(9)
C(15)–C(24) 1.380(3)	C(41)–Sb(2)–C(53) 109.46(9)
C(15)–C(16) 1.413(3)	C(59)–Sb(2)–C(53) 106.29(9)
C(16)–C(17) 1.385(3)	
C(17)–C(18) 1.393(3)	
C(18)–C(23) 1.408(3)	
C(18)–C(19) 1.531(3)	
C(19)–C(20) 1.534(4)	
C(20)–C(21) 1.252(5)	
C(21)–C(22) 1.462(6)	
C(22)–C(23) 1.533(4)	
C(23)–C(24) 1.401(3)	

Table 2
Crystallographic data on **3**·CHCl₃.

Empirical formula	C ₆₅ H ₆₇ Cl ₃ O ₄ Sb ₂
Formula weight	1262.04
Temperature (K)	100(2)
Wavelength (Å)	0.71073
Crystal system	Monoclinic
Space group	P2 ₁ /c
<i>Unit cell dimensions</i>	
<i>a</i> (Å)	15.6219(3)
<i>b</i> (Å)	15.7189(3)
<i>c</i> (Å)	23.4812(4)
α (°)	90.00
β (°)	93.861(2)
γ (°)	90.00
Volume (Å ³)	5752.94(18)
<i>Z</i>	4
<i>D</i> _{calc} (Mg/m ³)	1.457
Absorption coefficient (mm ⁻¹)	1.126
<i>F</i> (0 0 0)	2568
Crystal size (mm ³)	1 × 0.5 × 0.1
Theta range for data collection (°)	3.04–28.28
Completeness to $\theta = 30.51$ (%)	99.8
Reflections collected	14252
Independent reflections	10827 [<i>R</i> _(int) = 0.0329]
Absorption correction	CrysAlis RED
Maximum and minimum transmission	0.827; 1
Refinement method	Full-matrix least-squares on <i>F</i> ²
Data/restraints/parameters	14252/0/672
Final <i>R</i> indices [<i>I</i> > 2 σ (<i>I</i>)]	<i>R</i> ₁ = 0.0295, <i>wR</i> ₂ = 0.0697
<i>R</i> indices (all data)	<i>R</i> ₁ = 0.0461, <i>wR</i> ₂ = 0.0725
Goodness-of-fit (GOF) on <i>F</i> ²	1.019



Scheme 1.

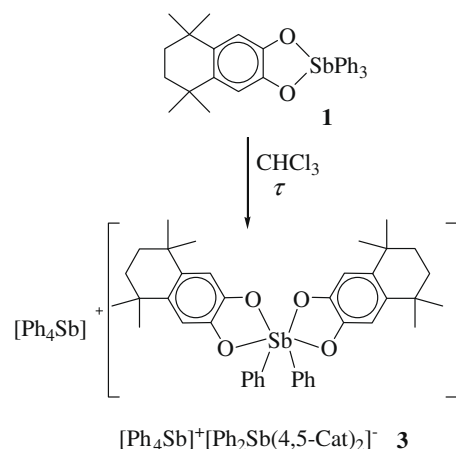
thylantimony analog **2** undergoes oxidation on air involving anti-mony-ethyl groups in oxidation.

We have found an interesting transformation of **1**: it transforms in polar solvent (we have used CHCl₃ or acetone) to a complex compound consisting of tetraphenylstibonium(V) cation and diphenyl-bis-catecholatoantimony(V) anion (**3**) (**Scheme 2**). This process in CDCl₃ requires 7 days at room temperature to be completed, but only 1 day in acetone.

The formation of complex **3** reverberates throughout NMR spectrum. **Fig. 1** shows ¹H NMR spectra of **1** and **3** in D-acetone. Catecholate **1** (as well as **2**) has a symmetrical structure (both aromatic protons of Cat ligand in **1** appear as one singlet with $\delta = 6.69$ ppm (d⁸-acetone), four methyl groups give rise to one singlet at 1.20 ppm and protons of both –CH₂– fragments of tetrahydronaphthalenecatecholate part also give singlet at 1.62 ppm). The formation of anion [Ph₂Sb(4,5-Cat)₂][–] causes the magnetic nonequivalence of all methyl groups – instead of one singlet one can observe four singlets at the region of 1.07–1.20 ppm. The signal from aromatic catecholate protons splits onto two singlets at 6.29 and 6.63 ppm. Tetraphenylantimony(V) cation appears as two multiplets at 7.68–7.85 ppm (*ortho*- and *para*-protons) and 7.89–7.96 (*meta*-protons). Interestingly, the singlet from CH₂ groups protons is only downshifted from 1.62 to 1.56 ppm.

¹³C NMR spectrum of **3** confirms the observations made from ¹H NMR spectra: methyl carbons form four singlets (32.51, 32.58, 32.61 and 32.78 ppm), CH₂ groups as well as carbons of –C(Me)₂– moieties become gently nonequivalent (36.72, 36.74 and 34.19, 34.21 ppm, respectively).

We have to note that such type reaction is well-known for anti-mony complexes. F.e. as we have reported previously, triphenylantimony(V) phenanthrene-9,10-diolate exists in equilibrium with ionic complex [Ph₄Sb][Ph₂Sb(PhenCat)₂] in toluene solution [19]. In the case of **1**, the rearrangement product **3** is much less soluble in chloroform (as well as in acetone) than initial catecholate **1** and there is no an equilibrium between **1** and **3**. The rearrangement is not reversible under the considered conditions.



Scheme 2.

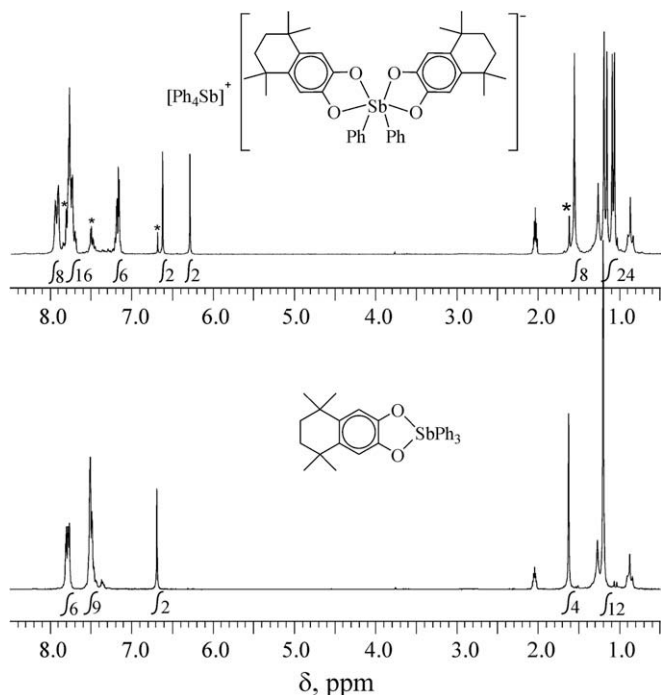


Fig. 1. ^1H NMR spectra of **3** (as the rearrangement product of **1** after 1 day, top) and **1** (bottom), D-acetone, 298 K. The asterisk in top spectrum shows residual signals from initial catechol **1**.

3.2. X-ray structure of **3**·CHCl₃

Complex **3** is a white crystalline powder which easily crystallizes from chloroform; this compound is only poorly soluble in non-polar solvents such as alkane, benzene, and toluene.

X-ray suitable crystals of **3** were grown in chloroform as the solvate **3**·CHCl₃. Fig. 2 shows the molecular structure of this complex.

An unit cell contains four $[\text{Ph}_2\text{Sb}(4,5\text{-Cat})_2]^-$ anions and four Ph_4Sb^+ cations. Antimony atom Sb(1) in anion has a slightly distorted octahedral structure and phenyl groups are *cis*-located with C(35)–Sb(1)–C(29) angle of $98.69(9)^\circ$. The dihedral angle between Sb(1)O(1)O(2) and Sb(1)O(3)O(4) planes is equal $84.46(9)^\circ$. At the same time, the angle formed by catecholate ligands' planes is $77.16(8)^\circ$. Five-atom chelate rings are slightly not planar, torsion angles O(1)C(1)C(2)O(2) and O(3)C(15)C(16)O(4) are $1.82(8)$ and $0.45(8)^\circ$, respectively.

The Sb(1)–O(1–4) bonds (Table 1) are in good agreement with the sum of covalent radii of the corresponding elements ($1.41 + 0.66 = 2.05 \text{ \AA}$ [28,29]). At the same time, these bond lengths reflect a weak trans-effect: Sb(1)–O(1) and Sb(1)–O(3) bonds (av. 2.0543 \AA) which are trans-positioned to phenyl groups are $\sim 0.03 \text{ \AA}$ longer than Sb(1)–O(2) and Sb(1)–O(4) bonds (av. 2.0245 \AA). Both chelating ligands reflect dianionic catecholate nature: C–O distances ($1.351(3)$ – $1.364(3) \text{ \AA}$) are typical for catecholates [18,20,30,31], the C–C bond lengths of six-membered carbon rings C(1–6) and C(15–24) vary in the range of $1.378(3)$ – $1.416(3) \text{ \AA}$ (av. 1.397 \AA) according to the lengths of aromatic C–C bonds.

Antimony Sb(2) atom in Ph_4Sb^+ cation is tetrahedral (average bond angle around Sb(2) atom is 109.45°), antimony-to-carbon bonds are very close and vary in the range 2.091 – $2.100(2) \text{ \AA}$ only.

One solvent chloroform molecule is coordinated to oxygen O(1) of Cat ligand in complex anion; the distance H(01)···O(1) is 2.15 \AA that is shorter than the sum of van der Waals radii (2.7 \AA) [28]. We have found an interesting interaction of phenyl's hydrogens H(44) and H(45) in tetraphenylantimony(V) cation with π -systems of catecholate and one phenyl rings in $[\text{Ph}_2\text{Sb}(4,5\text{-Cat})_2]^-$ anion (Fig. 3). The distance "H(44)···center of phenyl ring C(35–40)" is $2.86(2) \text{ \AA}$, H(44)···carbons C(35–40) bonds lie in the range $3.13(2)$ – $3.22(2) \text{ \AA}$. In the case of H(45), the distance "H(45)···center of phenyl ring C(1–4,9,10)" is $2.61(2) \text{ \AA}$ and H(45)···C(1–4,9,10) distances are $2.77(2)$ – $3.12(2) \text{ \AA}$. The analogical C–H··· π -system interactions ($<3.05 \text{ \AA}$) were discussed by Nishio [32].

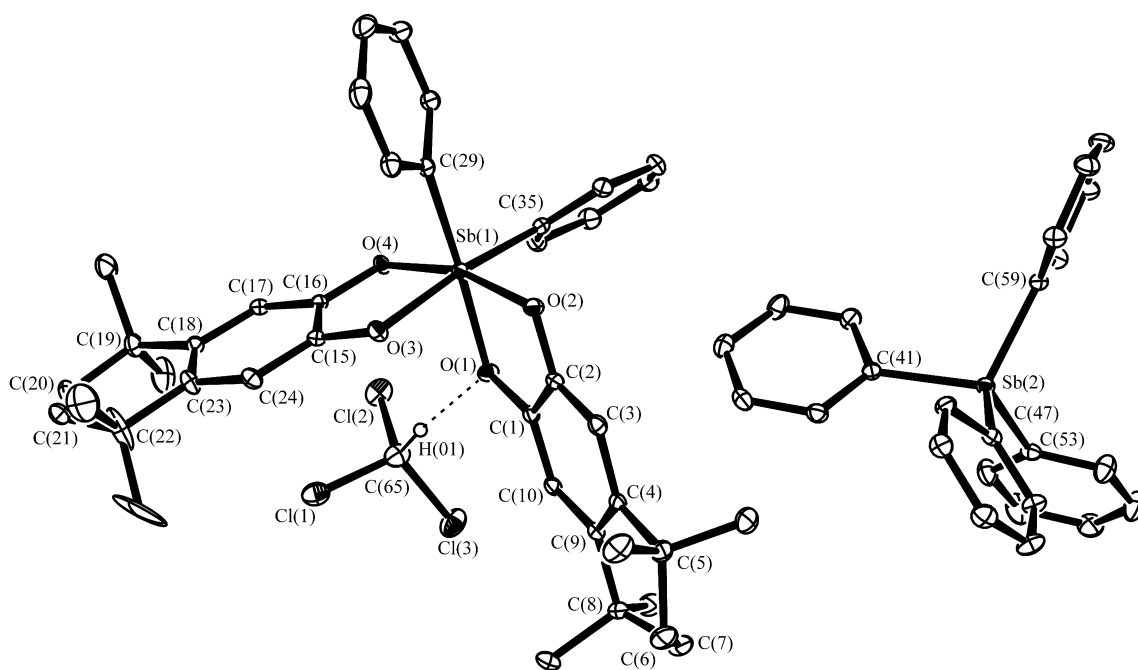


Fig. 2. The molecular structure of **3**·CHCl₃ (an ORTEP plot, 50% probability ellipsoids).

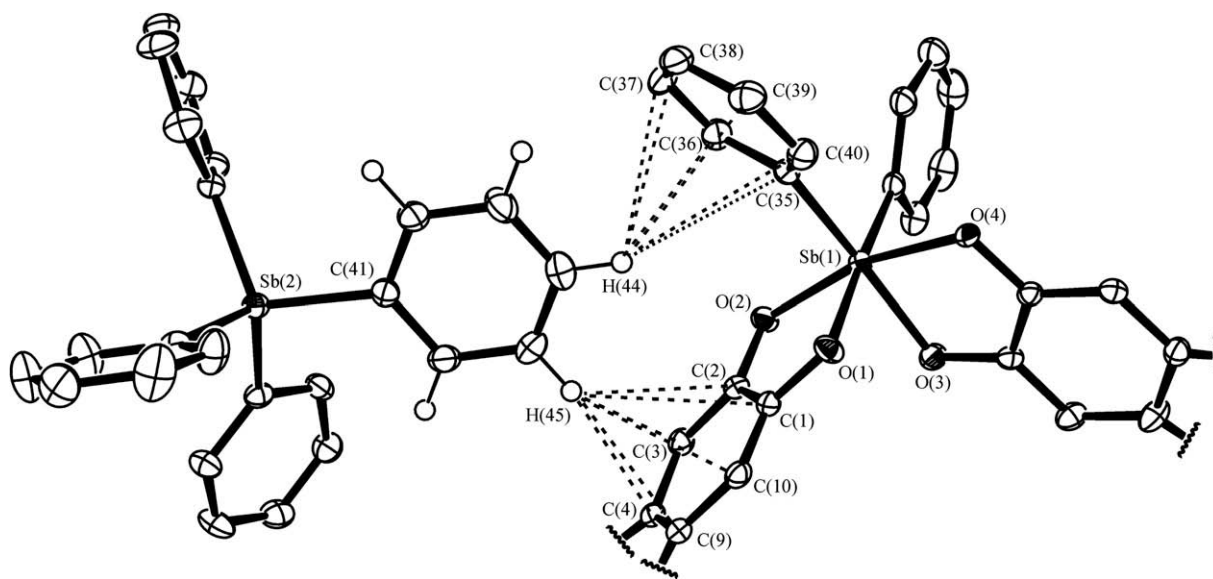


Fig. 3. The molecular structure of **3**·CHCl₃ (an ORTEP plot, 50% probability ellipsoids). The chloroform molecule, carbons C(5)–C(8), C(11)–C(14), C(19)–C(22), C(25)–C(28), hydrogens (excepting H(42)–H(46)) are omitted for clarity.

Table 3
Redox-potentials of antimony(V) catecholato complexes.

Compound	$E_{1/2}^1$ (V)	I_c/I_a	n	$E_{1/2}^2$ (V)	I_c/I_a	n
Ph ₃ Sb(3,6-DBCat) [21]	0.89	0.80	1	1.40 irr.	0.5	1
1 Ph ₃ Sb(4,5-Cat)	0.75	0.65	1	1.41	–	<1
2 Et ₃ Sb(4,5-Cat)	0.64 ^a	–	1	0.91	–	–
3 [Ph ₄ Sb][Ph ₂ Sb(4,5-Cat) ₂]	0.49	0.85	1	0.97 ^b	0.67	1.5

Conditions: CH₂Cl₂, $V = 0.2 \text{ V s}^{-1}$, glassy carbon working electrode, Ag/AgCl/KCl reference electrode, 0.1 M (*n*-Bu₄N)ClO₄, $C_{\text{complex}} = 2 \times 10^{-3} \text{ M}$, Ar, n -number transferring electrons vs. internal standard – ferrocene; I_c/I_a – currents ratio.

^a Peak potential.

^b $E_{1/2}^1$.

3.3. Electrochemistry

As we have shown previously, the first redox-potential of triphenylantimony(V) catecholato complexes plays an important role in dioxygen binding process where a key stage of dioxygen addition is an one-electron oxidation of dianionic catecholato ligand to radical-anionic o-semiquinonate by dioxygen [21]. To ascertain the electrochemical properties of complexes **1–3**, and to understand the influence of structural features as well as effect of substituents at antimony atom (f.e. Ph₃Sb and Et₃Sb) on redox-behavior, we have performed the electrochemical investigations.

Cyclic voltammograms have been recorded in CH₂Cl₂ solutions of complexes containing 0.10 M (*n*-Bu₄N)ClO₄ as supporting

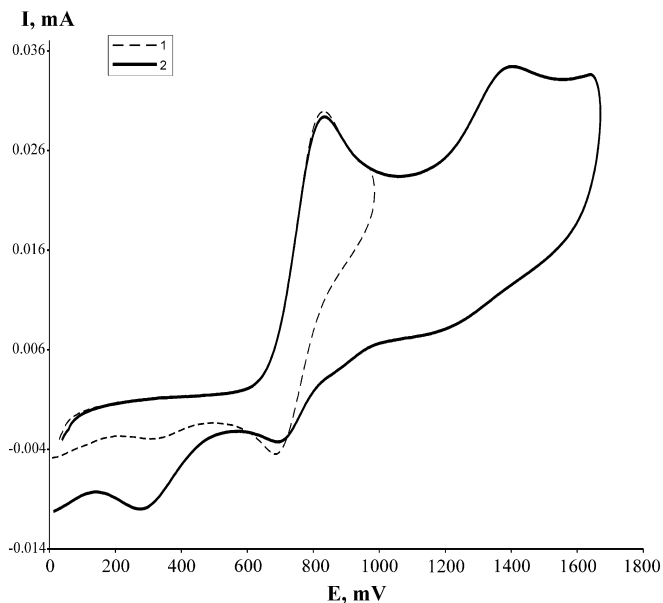


Fig. 4. CV of complex **1** (CH₂Cl₂, glassy carbon electrode, Ag/AgCl/KCl reference electrode, 0.1 M [*n*-Bu₄N]ClO₄, $C = 2 \times 10^{-3} \text{ M}$, under argon). The potential range extension 1.0 V (line 1) and 1.7 V (line 2).

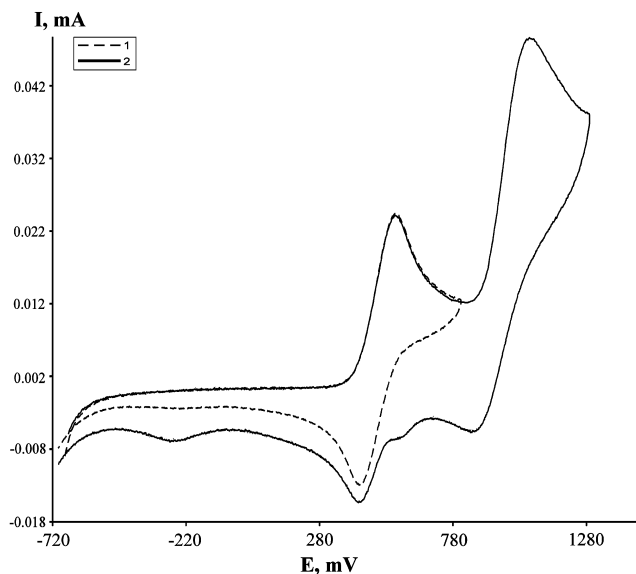
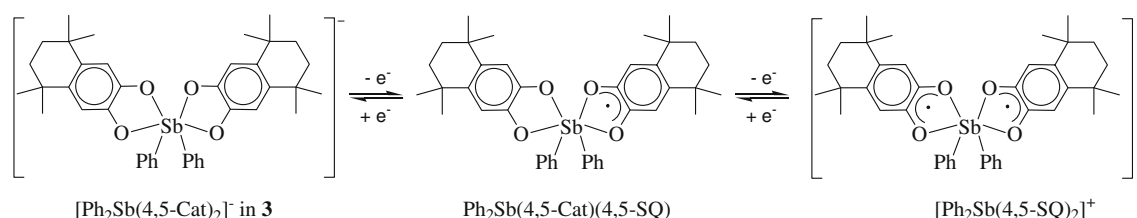


Fig. 5. CV of complex **3** (CH₂Cl₂, glassy carbon electrode, Ag/AgCl/KCl reference electrode, 0.1 M [*n*-Bu₄N]ClO₄, $C = 2 \times 10^{-3} \text{ M}$, under argon). The potential range extension 0.8 V (line 1) and 1.3 V (line 2).



Scheme 3.

electrolyte at a glassy carbon working electrode and a Ag/AgCl/KCl reference electrode. Table 3 summarizes electrochemical results.

The CV of $\text{Ph}_3\text{Sb}(4,5\text{-Cat})$ displays first reversible one-electron-oxidation wave at $E_{1/2}^1 = 0.75$ V (vs. Ag/AgCl) and second irreversible oxidation wave at $E_{1/2}^1 = 1.41$ V (Fig. 4). The observed values of potentials are close to earlier investigated $\text{Ph}_3\text{Sb}(3,6\text{-DBCat})$ [21]. At given scan rate, the number of electrons transferred during redox-process, has been estimated versus the one-electron current of ferrocene. The central Sb atom has the highest oxidation state and consequently all observed redox activity can be ascribed to ligand-based processes. The first reversible oxidation (Fig. 4 (1)) process represent the transition $(4,5\text{-Cat})/(4,5\text{-SQ})$ of coordinated ligand with formation cationic species $[\text{Ph}_3\text{Sb}(4,5\text{-SQ})]^+$. In the case of 4,5-dialkylsubstituted catecholate **1**, the first oxidation potential is shifted to cathode area by 0.14 V implicating easier oxidation of **1** in comparison with $\text{Ph}_3\text{Sb}(3,6\text{-DBCat})$. The current ratio points out the lowering stability of the generated cation against $[\text{Ph}_3\text{Sb}(3,6\text{-DBCat})]^+$. The extra reduction waves are fixes on the back scan of CV. They denote: the chemical stage occurs after electron transfer. The potential range extension before 1.7 V leads to the second irreversible oxidation process (Fig. 4 (2)) corresponding to the transition $\text{Ph}_3\text{Sb}(4,5\text{-SQ})^+/\text{Ph}_3\text{Sb}(4,5\text{-Q})^{2+}$. This redox stage is irreversible due to the decoordination of neutral quinone from central antimony atom.

The replacement of phenyl substituents with ethyl groups changes significantly electrochemical behavior of $\text{Et}_3\text{Sb}(4,5\text{-Cat})$ (**2**) (Table 3). The two oxidation processes have irreversible manner. The intermediates being formed from compound **2** in the redox stages are unstable in time scale of CV experiment. The donor influence of the alkyl radicals causes the drift of oxidation potential toward cathode area by 0.18 V. The first oxidation leads to complex decomposition: the reaction is accompanied by the evaluation of gaseous product on the surface of working electrode, while the *o*-quinone, as the product of disproportionation of *o*-semiquinone, forms in the minor values. Evidently electron transfer initiates break down of weak bond Sb–C [33] leading to ethyl radical abstraction and its subsequent reactions: recombination on the electrode surface or with solvent. The second oxidation process increases the wave of *o*-quinone on the reverse scan. Consequently, alkyl donor radicals at heavy antimony atom decreases the stability of $\text{R}_3\text{Sb}(\text{Cat})$ complexes appreciably.

Bis-chelate transition metal complexes with catecholate ligands containing donor alkyl substituents are very sensitive to the air and have low redox-potentials transition $(\text{Cat})/(\text{SQ})$ [34]. Heavy antimony atom in high oxidation state stabilizes bis-catecholate form in complex **3**, which undergoes oxidation process in positive potential range. The CV of $[\text{Ph}_4\text{Sb}][\text{Ph}_2\text{Sb}(4,5\text{-Cat})_2]$ displayed two reversible oxidation stages (Fig. 5).

The first process at 0.49 V (Fig. 4 (1)) is one-electron reversible transition monoanion to neutral complex $[\text{Ph}_2\text{Sb}(4,5\text{-Cat})(4,5\text{-SQ})]$. Noteworthy, the coordination of second Cat ligand to antimony (in anion $[\text{Ph}_2\text{Sb}(4,5\text{-Cat})_2]^-$) results in the redox-potential $E_{1/2}^1$ shift to cathode area. The oxidized form $[\text{Ph}_2\text{Sb}(4,5\text{-Cat})(4,5\text{-SQ})]$ is quite stable and we have no found decomposition products. The second

oxidation process ($E_{1/2}^1 = 0.97$ V) is quasi reversible and the number of electrons participating in electrochemical reactions is more than one (Fig. 4 (2)). It seems to be due to the consequent reaction of doubly oxidized adduct leading to its decomposition. The reverse scan of CV shows the appearance of peaks from decomposition products. Cationic species $[\text{Ph}_2\text{Sb}(4,5\text{-SQ})_2]^+$ containing two *o*-semiquinone radical anion ligands are unstable and ligands are decoordinates. In fact, one-electron oxidized neutral form $\text{Ph}_2\text{Sb}(4,5\text{-Cat})(4,5\text{-SQ})$ is electrochemically accessible while next oxidation step causes complex destruction. The scheme of redox transformations is shown on Scheme 3.

We have studied the possibility of chemical generation of the oxidized forms for **1** and **3** using EPR technique. The oxidation of **3** by $[\text{Fc}]\text{PF}_6$ in CH_2Cl_2 leads to paramagnetic $[\text{Ph}_2\text{Sb}(4,5\text{-Cat})(4,5\text{-SQ})]$ which has an isotropic EPR spectrum at room temperature with $g_i = 2.0037$ and spectrum extension of 4.5 G without any observable hyper-fine structure. At the same time, complex **1** is not oxidized by $[\text{Fc}]\text{PF}_6$ that is in agreement with electrochemical data. However, the oxidation of **1** by silver(I) triflate yields $[\text{Ph}_3\text{Sb}(4,5\text{-SQ})]^+$ cation, its EPR spectrum is unresolved broadened multiplet with $g_i = 2.0040$ and the spectrum extension of 6.8 G.

4. Conclusions

The new catecholate complexes (4,5-(1,1,4,4-tetramethyl-butane-1,4-diyl)-catecholato)-triphenylantimony(V) (**1**) and (4,5-(1,1,4,4-tetramethyl-butane-1,4-diyl)-catecholato)-triethylantimony (V) (**2**) were synthesized by the oxidative addition of 4,5-(1,1,4,4-tetramethyl-butane-1,4-diyl)-*o*-benzoquinone to triphenyl/triethylstibine. In polar solvents the first complex transforms easily to ionic compound **3** containing $[\text{Ph}_4\text{Sb}]^+$ cation and $[\text{Ph}_2\text{Sb}(4,5\text{-Cat})_2]^-$ anion. All complexes exhibit a series of oxidation waves on CV. Complexes **1** and **3** are air-stable while **2** slowly decomposes on air in solution that is in agreement with the redox-potentials of these complexes. Under the oxidation complexes **1** and **3** form quite stable paramagnetic *o*-semiquinonato species $[\text{Ph}_3\text{Sb}(4,5\text{-SQ})]^+$ and $[\text{Ph}_2\text{Sb}(4,5\text{-SQ})(4,5\text{-Cat})]$.

Acknowledgements

We are grateful to the Russian Foundation for Basic Research (Grants 07-03-00819, 07-03-00711, 09-03-00677), the presidium of RAS (the subprogram "Molecular Design of Magnetoactive Substances and Materials"), President of Russian Federation (Grants NSH-4182.2008.3, MK-1286.2009.3) and Russian science support foundation (A.I. Poddel'sky) for financial support of this work.

References

- [1] J.P. Finet, Ligand Coupling Reactions with Heteroatomic Compounds, Pergamon, New York, 1998, p. 308.
- [2] M. Fujiwara, M. Imada, A. Baba, H. Matsuda, Tetrahedron Lett. 30 (1989) 739–743.
- [3] R. Nomura, T. Nakano, Y. Yamada, H. Matsuda, J. Org. Chem. 56 (1991) 4076–4077.

- [4] R. Nomura, Y. Hasegawa, M. Ishimoto, *J. Org. Chem.* 57 (1992) 7339–7341.
- [5] S.K. Kang, H.C. Ryu, Y.T. Hong, *J. Chem. Soc., Perkin Trans. 1* (2001) 736–739.
- [6] I.P. Beletskaya, A.V. Cheprakov, Metal complexes as catalysts for C–C cross-coupling reactions, in: M.D. Ward (Ed.), *Comprehensive Coordination Chemistry II: Applications of Coordination Chemistry*, vol. 9, 2003, pp. 305–360 (Chapter 9.6).
- [7] M. Fujiwara, A. Baba, H. Matsuda, *Chem. Lett.* (1989) 1247–1250.
- [8] L.-J. Zhang, Y.-Z. Huang, H.-X. Jiang, J. Duan-Mu, Y. Liao, *J. Org. Chem.* 57 (1992) 774–776.
- [9] Y.-Z. Huang, C. Chen, Y. Shen, *J. Organomet. Chem.* 366 (1989) 87–93.
- [10] A.V. Gushchin, E.V. Grunova, D.V. Moiseev, O.S. Morozov, A.S. Shavyrin, V.A. Dodonov, *Russ. Chem. Bull.* 52 (2003) 1376–1379.
- [11] A.V. Gushchin, D.V. Moiseev, V.A. Dodonov, *Russ. Chem. Bull.* 50 (2001) 1291–1294.
- [12] L.-J. Zhang, Y.-Z. Huang, L.-H. Huang, *Tetrahedron Lett.* 32 (1991) 6579–6582.
- [13] L.-J. Zhang, X.-S. Mo, J.-Z. Huang, Y.-Z. Huang, *Tetrahedron Lett.* 34 (1993) 1621–1624.
- [14] J. Reglinski, Environmental and medicinal chemistry of arsenic, antimony and bismuth, in: N.C. Norman (Ed.), *The Chemistry of Arsenic, Antimony and Bismuth*, Blackie, London, 1998 (Chapter 8).
- [15] U. Wormser, I. Nir, Pharmacology and toxicology of organic bismuth, arsenic and antimony compounds, in: S. Patai (Ed.), *Chemistry of Organic Arsenic, Antimony and Bismuth Compounds*, Wiley, New York, 1994, pp. 715–723 (Chapter 18).
- [16] S. Maeda, Synthesis of organoantimony and organobismuth compounds, in: S. Patai (Ed.), *Chemistry of Organic Arsenic, Antimony and Bismuth Compounds*, Wiley, New York, 1994, pp. 725–759 (Chapter 20).
- [17] G.A. Abakumov, A.I. Poddel'sky, E.V. Grunova, V.K. Cherkasov, G.K. Fukin, Yu.A. Kurskii, L.G. Abakumova, *Angew. Chem., Int. Ed.* 44 (2005) 2767–2771.
- [18] G.A. Abakumov, V.K. Cherkasov, E.V. Grunova, A.I. Poddel'sky, L.G. Abakumova, *Dokl. Chem.* 405 (2005) 222–224.
- [19] V.K. Cherkasov, G.A. Abakumov, E.V. Grunova, A.I. Poddel'sky, G.K. Fukin, E.V. Baranov, Yu.A. Kurskii, L.G. Abakumova, *Chem. Eur. J.* 12 (2006) 3916–3927.
- [20] V.K. Cherkasov, E.V. Grunova, A.I. Poddel'sky, G.K. Fukin, *J. Organomet. Chem.* 690 (2005) 1273–1281.
- [21] A.I. Poddel'sky, I.V. Smolyaninov, Yu.A. Kurskii, N.T. Berberova, V.K. Cherkasov, G.A. Abakumov, *Russ. Chem. Bull.* 3 (2009) 520–525.
- [22] D.D. Perrin, W.L.F. Armarego, D.R. Perrin, *Purification of Laboratory Chemicals*, Pergamon, Oxford, 1980.
- [23] K. Issleib, B. Hamman, *Z. Anorg. Allg. Chem.* 339 (1965) 289.
- [24] V.A. Garnov, V.I. Nevodchikov, L.G. Abakumova, G.A. Abakumov, V.K. Cherkasov, *Dokl. Akad. Nauk SSSR* 15 (1987) 1864–1866 (in Russian).
- [25] G.M. Sheldrick, *Acta Crystallogr.* A64 (2008) 112–122.
- [26] L.J. Farrugia, *J. Appl. Crystallogr.* 32 (1999) 837–838.
- [27] C. Katayama, *Acta Crystallogr.* A42 (1986) 19–23.
- [28] S.S. Batsanov, *Russ. J. Inorg. Chem.* 36 (1991) 3015–3037.
- [29] J. Emsley, *The Elements*, Clarendon Press, Oxford, 1991.
- [30] C.G. Pierpont, *Coord. Chem. Rev.* 219–221 (2001) 415–433.
- [31] C.G. Pierpont, *Coord. Chem. Rev.* 216–217 (2001) 99–125.
- [32] M. Nishio, *Cryst. Eng. Commun.* 6 (2004) 130–158.
- [33] W. Levason, G. Reid (Eds.), *Comprehensive Coordination Chemistry II: Coordination Chemistry of the s, p, and f Metals*. 3.6. Arsenic, Antimony, and Bismuth, vol. 3, 2003, pp. 465–544.
- [34] P. Zanello, M. Corsini, *Coord. Chem. Rev.* 250 (2006) 2000–2022.